High-Efficiency X-Band MMIC GaN Power Amplifiers with Supply Modulation

Andrew Zai, Dongxue Li, Scott Schafer, and Zoya Popovic
University of Colorado - Boulder
Room ECEE1B55, 425 UCB
Boulder, CO 80309-0425
andrew.zai@colorado.edu, dongxue.li@colorado.edu,
scott.r.schafer@colorado.edu, zoya.popovic@colorado.edu

***Abstract*— This paper presents measurement results on supply-modulated X-band 0.15μm gate width GaN HEMT MMIC power amplifiers for OFDM signals. Two PAs at 10GHz with 4 and 10W output powers show peak CW efficiencies of 69% and 55%, with gains of 8.5 and 20.4 dB respectively. Supply modulation trajectories are designed by static characterization of each MMIC PA, and the drain modulation is performed though both a linear broadband modulator and a high-efficiency 5-MHz switching modulator. The PAs are tested in four modes: (1) with a constant 20-V supply and the 18-MHz OFDM signal input through the drive; (2) pure envelope tracking; (3) signal-split supply modulation; and (4) envelope elimination and restoration (EER) with a 5-MHz switching modulator. Average PAE and composite power added efficiencies are compared, reaching 65.4% and 35%, respectively, with the 4-W PA and a linear modulator.**

***Index Terms*— power amplifier, envelope tracking, efficiency, GaN, MMIC**

I. Introduction

Spectrally-efficient signals with high peak-to-average power ratios (PAPR) are difficult to amplify with high average efficiency, and a number of transmitter architectures, such as Doherty [1], outphasing PAs [2] and envelope tracking [3], have been developed to solve this problem. Supply modulation has been demonstrated with high efficiencies up to the 2-GHz range with WCDMA and LTE signals [4]. At X-band, slow supply modulation with sub-watt GaAs PAs has been demonstrated with CPAE>60% [5]. All these architectures involve additional hardware compared to a single PA and it is important to quantify the gain in efficiency and weigh it against the added complexity. In this paper, we discuss measurements of composite efficiency of GaN MMIC PAs combined with a supply modulator (SM), Fig.1. The signal is digitally split into two envelope components $A_1(t)$ and $A_2(t)$ and a phase $\phi(t)$, where A_1 is input through the supply modulator and its value is determined based on static PA characterization and the probability density function of the signal envelope.

Integrated design of the PA and SM is essential not only for optimizing transmitter performance, but also for ensuring stability, as described in detail in [6]. In the MMICs shown in Fig.1, the drain impedance at envelope bandwidth is measured and the circuit, bias lines and interconnect to SM are designed and modeled to ensure stability, specifically by minimizing capacitance. The PAs are designed in the TriQuint 0.15μm GaN process. The 4-W PA has a single-stage with 8.5-dB of gain, biased in class-B with a peak PAE= 69%. The 10-W PA is a two-stage power-combined 20.4-dB gain PA biased in class-AB with a peak PAE=55%.

The results in this paper present a comparison study for the PAs tested in four modes: (1) with a constant 20-V supply and the 18-MHz OFDM signal input through the drive; (2) pure envelope tracking (ET); (3) signal-split supply modulation; and (4) envelope elimination and restoration (EER) with a 5-MHz switching modulator.

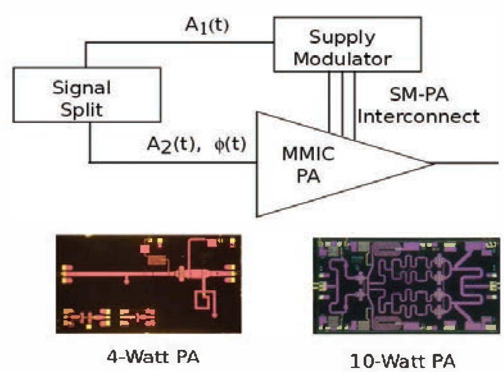

Fig. 1. Block diagram of a supply-modulated PA. . The signal is digitally divided into two envelope components $A_1(t)$ a $A_2(t)$ and a phase $\phi(t)$, and A_1/A_2 can be varied. Two MMICs shown in the photographs are tested in this configuration with two types of supply modulators.

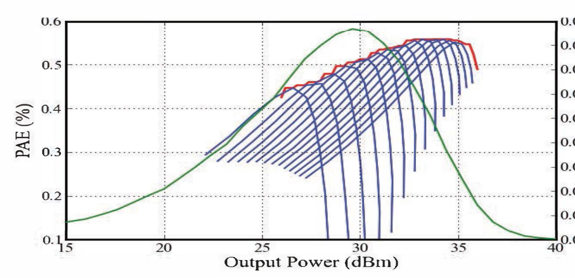

Fig. 2. The PAE of this power amplifier for voltages swept from 7-20 Volts (blue) with the maximum PAE trajectory (red). The PDF of the desired output OFDM signal is shown in green with the probability displayed on the right.

II. Experimental Setup

In order to determine A_1 and A_2, the MMICs are characterized statically with regard to output power, gain, and efficiency. The first step after standard MMIC PA characterization is to

978-1-4799-3869-8/14/$31.00 ©2014 IEEE

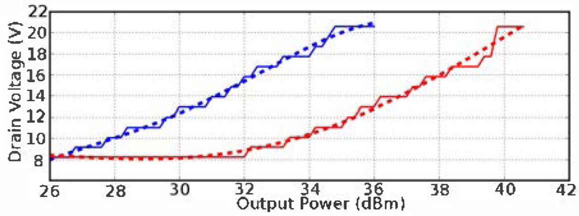

Fig. 3. The trajectories for the 4-W PA (blue) and 10-W PA (red).

design the drain supply voltage versus desired output power, referred to as the trajectory. As an example, the 4-W MMIC static characterization curves are shown in Fig. 2 (blue lines). The pdf for output power of an LTE-like OFDM signal is superimposed (green), and a curve following peak efficiency over drain supply voltages can be synthesized (red). Similar plots can be obtained for the 10-W MMIC. Based on the static characterization, trajectories of $V_{dd}(P_{out})$ are designed as a polynomial fit for each PA, shown in Fig. 3 in dashed line.

In the experimental setup of Fig. 4, the signal modified by the trajectory is provided by the two arbitrary waveform generators (Agilent N8241A), which are replaced by an FPGA in the switching SM tests. The drive signal is I/Q upconverted by a RF signal generator (Agilent E8267D PSG) and amplified by a 40-dB gain driver amplifier (Microwave Amps AM53-9.5-10.5-30-40). A signal analyzer (Agilent N9030A PXA) is used to analyze both spectral and time-domain properties of the input and output MMIC PA signals mounted in a low-loss fixture which can accommodate a variety of chip sizes with easy replacement.

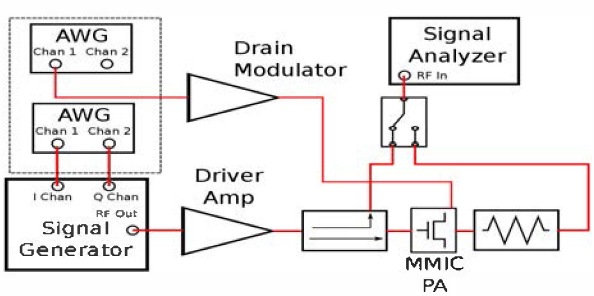

Fig. 4. Interconnection of test equipment and supply modulation components used in this experiment. The measurements with the linear modulator include the AWGs enclosed in the dashed box. These are replaced by an FPGA developement board in the switching modulator measurements.

A linear supply modulator is implemented with off-the-shelf electronic components as a 3-stage opamp with a final stage source-follower GaN packaged device (TriQuint T1G6003028-FS), which can be biased up to 30V but is limited to a 7-20V range in the experiments presented here. This SM was not designed for high-efficiency, but rather for linearity, and its efficiency is waveform-dependent and in the range of 50% for the OFDM waveforms used in this work. The output waveform of the SM needs to be precisely aligned with the drive signal in order to obtain minimal distortion in the output signal [7]. In the setup described in Fig.4, a radar-type waveform shown in Fig. 5 is used for alignment. The waveform is a linear FM modulation with a Gaussian envelope. Prior to alignment, the Gaussian envelope is mis-aligned with the zero-frequency point of the chirp. The alignment is performed by delaying the RF signal until the derivative of the phase is zero, as is the normalized magnitude of the output. This is illustrated in Fig. 5 (center) which gives an optimal delay of 152 ns. The final aligned signal is shown in Fig. 5 (bottom).

Tests were also performed with a 5-MHz high-efficiency switching modulator, also implemented with off-the-shelf components as a PWM-driven Buck circuit. The PWM signals are provided by an Altera TR4 development board with 20-MHz switching speed. The efficiency of this modulator measured with a constant real load is 92% [8]. With the switcher testing, the AWGs are replaced with the FPGA (dashed line in Fig. 4), and in this case a different time-alignment technique still needs to be developed.

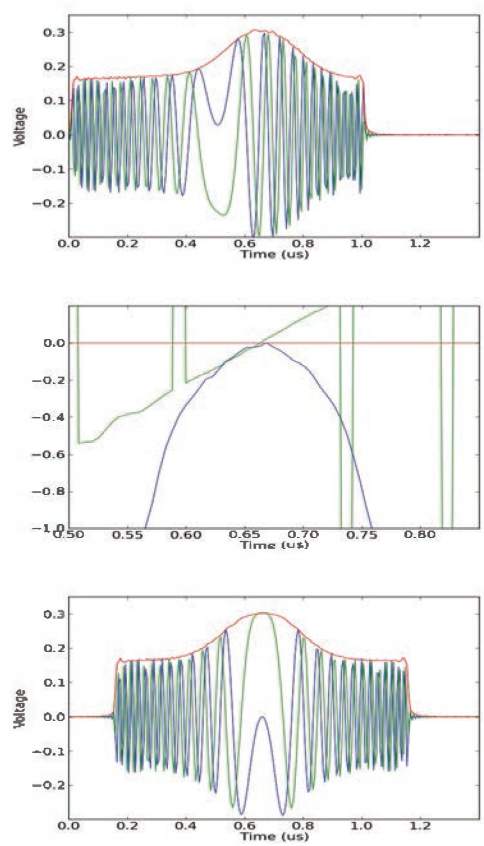

Fig. 5. The IQ output from the PA before alignment (top), the magnitude and derivative of phase used to align the signal paths (middle), and aligned IQ output after alignment is performed.

III. Measurements with an OFDM Signal

A. Linear Modulator with 15 MHz Bandwidth

The linear modulator bandwidth tested with a constant real load is about 50MHz, but the PA is a dynamic complex

TABLE I
SUMMARY OF RESULTS WITH 4-WATT PA

	Constant Supply	Modulated Supply	Signal Split	EER
Channel Power (dBm)	30.6	28.6	28.5	30.8
Peak Power (dBm)	36.3	36.5	36.5	35.5
Gain (dB)	8.5	6.4	6.4	-
PAE	43.9%	65.4%	62.6%	-
CPAE	43.9%	34.8%	33.1%	35.8%
$\eta_{Composite}$	-	-	-	60.4%
Drain Current (mA)	108.0	75.6	80.2	83.6
ACPR (dB)	-27.1	-23.3	-28.0	-

impedance, limiting the stable bandwidth to slightly above 15 MHz, and the signal envelope was filtered to meet the stability by monitoring the Bode plot of the SM with the PA connected.

Fig. 6 shows measured spectra at the output of the 4-W MMIC integrated with the linear supply modulator. As the drain voltage decreases, the gain of the 4-W PA compresses. When the trajectory envelope information is input completely through the SM, the linearity is degraded w.r.t. the constant drain supply case, as expected [6]. After a signal split is applied using a look-up table derived from static gain measurements, the ACPR improves and can now be more easily linearized using DPD. Table I compares the constant supply, envelope tracking and signal split cases for the 4-W MMIC PA with the linear modulator. Here the PAE is the average PA efficiency over the signal pdf, while the CPAE is the total efficiency including the fixture losses, supply modulator efficiency and PA efficiency, defined as:

$$PAE = \frac{\int P_{out}\,dt - \int P_{in}\,dt}{\int V_{ds}\,dt \int I_{ds}\,dt} \quad (1)$$

$$CPAE = \frac{\int P_{out}\,dt - \int P_{in}\,dt}{V_{DD} \int I_{ds}\,dt} \quad (2)$$

where V_{DD} is the bias of the supply modulator. These equations are used because our setup does not provide access to time domain current data, only the average current. The supply modulation improves the efficiency by 20% but degrades the ACPR, while the signal split improves the ACPR with minimal impact on efficiency. The CPAE is lower than that for the constant bias case, as expected because the SM is linear and shapes the drain waveform by dissipating power.

Table II shows the results with the 10-W MMIC. In this case, the signal split does not provide additional benefit, because the PA design is such that the trajectory follows constant gain contours. In this two-stage PA with only final-stage supply modulation, and with the inefficient linear supply modulator, the CPAE nevertheless increases to 23% from the 13% efficiency for a constant 20-V supply.

B. EER with a 5-MHz Switching Modulator

Since the linear supply modulator is inefficient, the 4-W PA is also characterized with the 5-MHz efficient switching modulator. In this case, envelope elimination and restoration (EER) is used initially, since this does not require time alignment. From Table I, the CPAE is 35.8%, which includes the losses of the SM. In this measurement, the input is always at peak power, which reduces overall efficiency. The composite drain efficiency, calculated as

$$\eta_{Composite} = \frac{\int P_{out}\,dt}{V_{DD} \int I_{ds}\,dt} \quad (3)$$

and is 60.4% in this case since it does not depend on the input drive. Given the PAE of the amplifiers and the efficiency of SM, the projected CPAE is above 55%. Achieving this requires time alignment, which is currently being implemented with the FPGA. To the best of the author's knowledge, this paper presents the highest combined efficiency, power level and bandwidth for integrated X-band supply-modulated PAs.

TABLE II
SUMMARY OF THE 10-W MMIC SUPPLY MODULATION RESULTS

	Constant Supply	Modulated Supply
Channel Power (dBm)	32.5	31.8
Peak Power (dBm)	40.3	40.3
Gain (dB)	20.4	19.6 dB
PAE	13.3%	41%
CPAE	13.3%	23.3%
Drain Current (mA)	282	255
ACPR (dB)	-26.2	-23.1

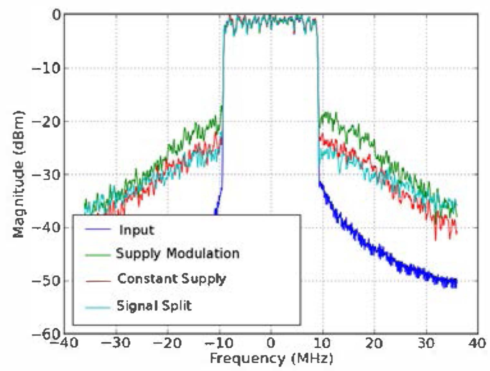

Fig. 6. Normalized power spectra of the input, modulated supply, signal split, and constant supply for the purposes of showing spectral regrowth.

ACKNOWLEDGMENT

This work was supported by the Office of Naval Research (ONR) under the Defense Advanced Research Projects Agency (DARPA) Microscale Power Conversion (MPC) Program under Grant N00014-11-1-0931.

REFERENCES

[1] B. Kim et al. "The Doherty power amplifier", *IEEE Microw. Mag.*, vol. 7, no. 5, pp.42 -50 2006

[2] M. P. van der Heijden et al. "A 19 W high-efficiency wideband CMOS-GaN class-E Chireix RF outphasing power amplifier", *IEEE MTT-S Int. Microw. Symp. Dig.*, pp.1 -4 2011

[3] J. Jeong et al. "High-efficiency WCDMA envelope tracking base-station amplifier implemented with GaAs HVHBTs", *IEEE J. Solid-State Circuits*, vol. 44, no. 10, pp.2629 -2639 2009

[4] D. F. Kimball et at. High-Efficiency Envelope-Tracking W-CDMA Base-Station Amplifier Using GaN HFETs, *IEEE Transactions on Microwave Theory and Techniques*, vol. 54, no. 11, pp. 38483856, Nov. 2006.

[5] Narisi Wang et al. ”60% efficient 10-GHz power amplifier with dynamic drain bias control,” *Microwave Theory and Techniques*, IEEE Transactions on , vol.52, no.3, pp.1077,1081, March 2004

[6] J. Hoversten et al. Codesign of PA, Supply, and Signal Processing for Linear Supply-Modulated RF Transmitters, *Microwave Theory and Techniques, IEEE Transactions on*, vol. 60, no. 6, pp. 20102020, 2012.

[7] Feipeng Wang et al. ”Design of wide-bandwidth envelope-tracking power amplifiers for OFDM applications,” *Microwave Theory and Techniques, IEEE Transactions on* , vol.53, no.4, pp.1244,1255, April 2005

[8] M. Rodriguez et al. ”High frequency PWM Buck converter using GaN-on-SiC HEMTs,” *IEEE Trans. on Power Electronics, 2014*, August 21, 2013.

978-1-4799-3869-8/14/$31.00 ®2014 IEEE